

Observation of a magnetic-field-induced resonance in the homogeneous dephasing time for the 1D_2 - 3H_4 transition in $\text{Pr}^{3+}:\text{YAlO}_3$

Baozhu Luo and S. Kröll

Department of Physics, Lund Institute of Technology (LTH), Box 118, S-221 00 Lund, Sweden

(Received 13 May 1996)

Using two-pulse photon echo excitation a strong resonance in the measured homogeneous dephasing time as a function of magnetic field is observed in the 3H_4 - 1D_2 transition of $\text{Pr}^{3+}:\text{YAlO}_3$. The resonance could only be observed at low excitation energies since it otherwise was masked by excitation intensity dependent extra dephasing processes in the crystal. Thus intensity dependent dephasing processes may not only affect the apparent dephasing time of a system but may also mask other more subtle interactions in the materials studied. It is reasonable to assume that the type of resonance observed could be caused by Zeeman induced level crossings in the active ion or in the host crystal ions or, possibly, that it could be due to coincidences between Zeeman level transition frequencies. However, based on current data of the $\text{Pr}:\text{YAlO}_3$ system the observed resonance could not be unambiguously tied to such effects. [S0163-1829(96)06238-8]

I. INTRODUCTION

Basic spectroscopic investigations on rare-earth and transition element doped inorganic crystals have for more than 30 years been stimulated by the (potential as well as existing) applications of these materials. In addition to studies of these materials due to their usefulness as active materials in solid-state lasers, many basic investigations are now also spurred by their interesting potential for frequency- or time-domain optical storage.¹⁻³ An often quoted figure of merit for such applications is the number of bits which theoretically can be addressed in a single spatial point by utilizing different absorption frequencies in the potential storage material. This figure of merit is given by the ratio between the inhomogeneous and homogeneous linewidths for the transitions used for the storage process. To optimize this figure of merit one would, for example, then identify transitions where the homogeneous linewidth is as narrow as possible.⁴ Although the homogeneous linewidth in principle is a well-defined physical quantity which can be measured once and for all for a certain transition and material, the values of the homogeneous linewidths in especially rare-earth-ion-doped systems have been revised many times over the years, see, e.g., Ref. 5. However, since the time when photon echoes started to be used for determining the homogeneous dephasing times demonstrating linewidths down to the kHz region,⁶ it has been felt that the issue of the homogeneous linewidth measurements in rare-earth-ion-doped crystals are under reasonable control. Current investigations have, for example, centered on obtaining the narrowest possible linewidths or on excitation pulse energy (intensity) dependent effects of the linewidth measurements, e.g., Refs. 4, 7-12. Such excitation pulse dependent dephasing effects are interesting because they tell us about the interaction between excited atoms and their neighborhood. They can, however, also be a disadvantage. For the storage applications mentioned above it is a significant problem since the increased dephasing rate corresponds to larger homogeneous linewidths and a lower figure of merit for the storage density.¹³ In this paper we

point out another disadvantage of the excitation-pulse-dependent dephasing, namely, that this effect may mask other fundamental interactions in the material. Here data that demonstrate a magnetic-field-induced interaction in Pr doped YAlO_3 that can only be observed at excitation pulse energies so small that the excitation energy-dependent contribution to the dephasing is negligible, are presented.

The interactions responsible for the linewidths in rare-earth-ion-doped inorganic materials where the rare-earth ion has an even number of electrons, as in Pr^{3+} , are generally expressed as (e.g., Ref. 12),

$$\Gamma(\text{total}) = \Gamma(\text{radiative decay}) + \Gamma(\text{ion-spin}) + \Gamma(\text{ion-ion}) + \Gamma(\text{phonons}). \quad (1)$$

The linewidth contribution from thermal phonons is absent at sufficiently low temperatures although optical excitation of a transition itself can generate monoenergetic phonons that can alter the dephasing process, e.g., Ref. 10. The experiments in this paper are carried out at 4 K where any contribution from thermally generated phonons is negligible. The first term in Eq. (1) comes from the intrinsic upper state radiative decay and sets a fundamental lower limit to the linewidth that can be observed. The second term describes the interaction between the rare-earth ion and the nuclear spins of the surrounding host ions and the third term describes the interaction between the rare-earth ions themselves. The second term can generally be decreased by applying a magnetic field to the crystal that suppresses the nuclear spin-flips of the host ions. The ion-ion term especially describes the excitation energy dependence of the dephasing process⁷ and is generally ascribed to instantaneous spectral diffusion, e.g., Refs. 8 and 11 although other processes can also be important in certain cases.^{9,10,14} The main aim of this paper is to illustrate that by using a low excitation pulse energy, thereby reducing the ion-ion interaction term, quite weak and, potentially, not previously observed interactions can also be detected.

In the next section the experimental setup is described. Section III describes the measurements. To discuss the cause of the magnetic field induced resonance a brief description of

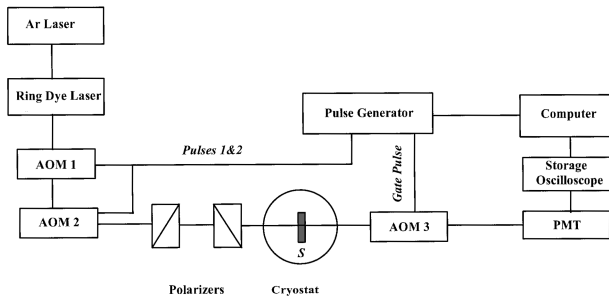


FIG. 1. The schematic diagram of the experimental apparatus. Acousto-optic modulator (AOM), Sample (S), Photo multiplier tube (PMT).

the magnetic field dependence of the hyperfine levels based on existing spectroscopic data is given in Sec. IV. Finally, the paper is concluded in Sec. V.

II. EXPERIMENT

Figure 1 shows a schematic diagram of the experimental apparatus. A Coherent CR699-21 ring dye laser pumped by a Spectra-Physics SP 171 Ar⁺ laser is used for the excitation. Two excitation pulses are generated by gating the dye laser radiation using two Isomet 1205C acousto-optic modulators in series. Two polarizers are placed in the front of the sample such that the excitation energy of the optical pulses can be continuously adjusted. The 1-mm-thick crystal of YAlO₃ doped with 0.1% Pr is placed in a liquid He cooled cryostat (Cryovac 100). The crystal is mounted with the crystal *c* axis along the laser beam propagation direction and with the *b* axis in the vertical direction. The polarization of the excitation light is parallel to the *b* axis. A pair of electromagnetic coils placed outside the cryostat generates a magnetic field ranging from 0 to 15 mT (0 to 150 G). The excitation pulses are focused into the crystal using a 15-cm lens, resulting in a focal area of about 10⁻⁴ cm². The pulse duration was 1 μs and the excitation power roughly ranged between 2 and 100 mW. Thus the energy fluence at the crystal was in the range 20 μJ/cm² to 1 mJ/cm². An additional acousto-optic modulator after the crystal is gated to open only at the time when the echo is emitted. The strong excitation pulses are thus attenuated about a factor of 1000 before reaching the photo multiplier tube (PMT) connected to a Tektronix 2431L digital storage oscilloscope. The photon echo signal is registered as a function of the separation between the first and second pulse in the two-pulse photon echo sequence. The timing of the excitation and detection pulses was controlled using four SRS DG135 delay generator cards inserted in a personal computer.

III. MEASUREMENTS

The photon echo signal is recorded versus the time separation of the two excitation pulses. An exponential decay curve is fitted to the experimental data using a least-squares fit and an apparent echo decay time is obtained. In the absence of intensity-dependent dephasing processes the echo decay time should be one fourth of the real homogeneous dephasing time, T_2 . A typical decay curve is shown in Fig. 2. The magnetic field is parallel to the crystal *c* axis. There is a

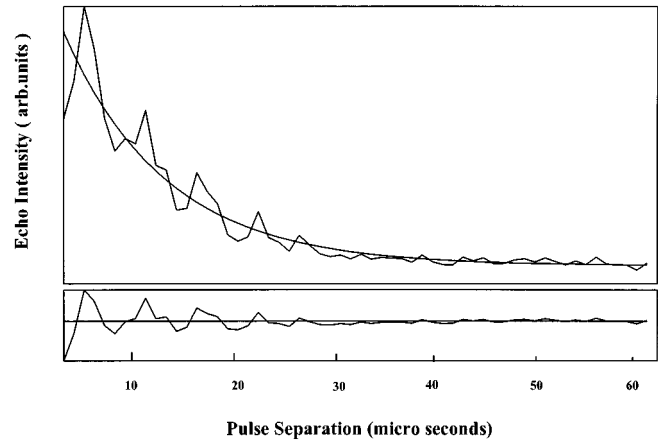


FIG. 2. Photon echo intensity decay curve versus pulse separation with a theoretical fit assuming a pure exponential decay. The magnetic field is 70 G and oriented parallel to the crystal *c* axis. The decay time is 10.3 μs and the modulation frequency seen in the decay curve is about 200 kHz. The lower part of the figure shows the deviation between the theoretical fit and the experimental data.

modulation superimposed on the decay curve. The modulation frequency varies with magnetic field and it is caused by quantum beats between Pr ¹D₂ excited state hyperfine Zeeman levels.¹⁵

The photon echo decay time is measured as a function of magnetic field for different excitation pulse energies and for different magnetic field orientations. Figure 3 shows the photon echo decay time versus magnetic field for excitation pulse energies of 2 and 17 nJ when the magnetic field is oriented parallel to the crystal *c* axis and for an excitation pulse energy of 2 nJ when the magnetic field is oriented perpendicular to the crystal *c* axis. For all excitation energies and both orientations the photon echo decay time first increases with magnetic field and then (for the range of magnetic fields studied) saturates. The reason that no data is plotted for the region between 0 to 40 G is that quantum beats between Zeeman sublevels make it difficult to obtain a reli-

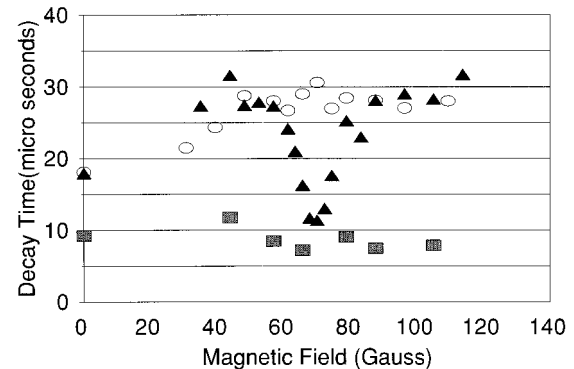


FIG. 3. Photon echo decay time as a function of magnetic field. Black triangles and grey rectangles represent excitation pulse energies of 2 and 17 nJ, respectively, when the magnetic field is oriented parallel to the crystal *c* axis. The open circle data corresponds to excitation pulse energies of 2 nJ when the magnetic field is oriented perpendicularly to the crystal *c* axis.

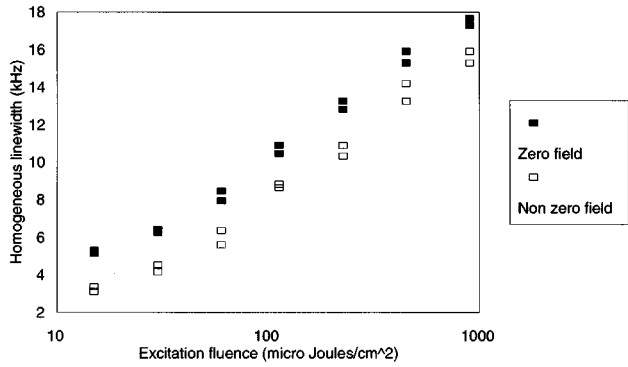


FIG. 4. Excitation fluence dependence of the homogeneous linewidth, with and without magnetic field.

able decay time. The increase in decay time is rather small at the higher excitation energy, since the reduction in the Γ (ion-spin) term in Eq. (1) is masked by the high value of the Γ (ion-ion) term, but at lower energy the decay time increases quite significantly. As can be seen there is a dip in the photon echo decay time as a function of increasing magnetic field when the field is oriented parallel to the c axis. The dephasing time then is essentially constant at least up to 150 G (not shown in the figure). In order to understand the origin of this resonance, measurements have been performed for the magnetic field oriented at 0, 5, 10, 20, 30, 45, and 90 degrees angle relative to the crystal c axis. The results show that the magnetic field induced resonance is most pronounced at an angle of 5° and 10° relative to the c axis and that it becomes broader and more shallow for the 20° and 30° cases. No resonance is observed for the 45° and 90° configurations. Possible origins of the resonance will be discussed in Sec. IV.

The investigation of the magnetic field induced resonance is also complemented with measurements of the excitation energy-dependent dephasing when the laser is tuned to the center as well as off the center of the absorption line. Figure 4 shows the apparent homogeneous linewidth as inferred from the decay time of the two-pulse photon echo measurements vs excitation fluence with zero magnetic field (black symbols) and with a field of 7 mT (open symbols). The field is oriented perpendicular to the c axis. The excitation energy dependence of the homogeneous dephasing time in Pr-doped YAlO_3 does not show the dominating asymmetry on the first and second pulse as is observed for the Eu and Tb systems.^{7,8} Thus instantaneous spectral diffusion, as it generally is described in these type of measurements,^{4,7,8,11,12,16} is not the main mechanism for the intensity dependence in Pr: YAlO_3 .^{9,10}

An external magnetic field breaks the energy degeneracy of antiparallel nuclear spins of equal magnitude and thus, for sufficiently large fields, inhibits the mutual spin flips of the Al ions reducing the Γ (ion-spin) term in Eq. (1). The radiative lifetime of the 1D_2 state is about 180 μs , e.g., Ref. 10. This gives a homogeneous linewidth contribution Γ (radiative) of about 0.9 kHz. From earlier magnetic field measurements⁶ the magnetic dipole interaction Γ (ion-spin) is estimated to 2.0 kHz. This is in good agreement with the part of the linewidth contribution that is eliminated in Fig. 4 by applying the magnetic field. As expected, Fig. 4 shows that

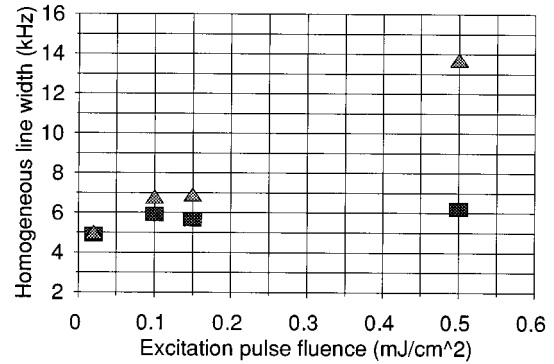


FIG. 5. Homogeneous linewidth as a function of excitation pulse energy at the peak of the absorption line (triangles) and 4 GHz off line center (rectangles).

the excitation energy-dependent dephasing contribution is independent of the magnetic field and therefore illustrates that this process involves neither the Al spin flips nor any other magnetic interaction.

In principle one could imagine that plain thermal heating from the laser pulses could have an effect on the dephasing. However, it is straight forward to show that the absorbed laser energy is insufficient to heat the sample any significant amount. The maximum energy absorbed per crystal atom and pulse can be expressed as (photon energy) \times (fraction of Pr ions within the laser bandwidth) \times (fraction of Pr ions in the crystal). If this is put equal to the increase in thermal energy per pulse, one obtains for the 3H_4 - 1D_2 transition $h\nu \times (1/5000) \times (0.001/5) = k\Delta T$, where $h\nu$ is the photon energy, k is Boltzmann's constant, and ΔT the temperature increase. At $\lambda=610.5$ nm, ΔT will only be around 0.5 mK per excitation pulse pair. Further, this value is most likely a severe over estimation since normally only a fraction of the electronic energy will be transformed into thermal energy through phonon interaction.

Figure 5 shows the excitation pulse energy dependence of the homogeneous linewidth at the center of the absorption line and 4 GHz off-line center. In this measurement, no magnetic field was applied. At the center of the inhomogeneous line profile the optical density (OD) equals 1.3. Assuming a Gaussian inhomogeneous line shape with a full width at half maximum of 5 GHz,⁵ then $\text{OD}=0.5$, 4 GHz off line center. Clearly the intensity dependent dephasing contribution is small when the absorption is small as has been observed previously.¹⁶ An apparent frequency dependence of the homogeneous linewidths have been observed previously, e.g., in Eu^{3+} -doped Y_2O_3 (Ref. 17) and $\text{EuP}_5\text{O}_{14}$.¹⁸ Originally the cause of the frequency dependence was analyzed in terms of a delocalization of the excitation and energy transfer within the inhomogeneous line. This effect was also described using the inhomogeneous line broadening theory developed later by Root and Skinner.¹⁹ In the Eu case above the doping concentration is rather high (2%). However, at a lower Eu concentration (0.25%) in YAlO_3 , no frequency dependence was observed.¹⁸ In our experiment, the Pr concentration is 0.1%, thus the frequency dependence in Fig. 5 is not readily attributed to delocalization of the excitation. Nevertheless, lately this description has not been used very extensively for

rare-earth-ion-doped crystals instead frequency and intensity-dependent homogeneous linewidths have been interpreted in terms of instantaneous frequency shifts of the excited atoms⁷ for, e.g., Eu^{3+} systems and in terms of excitation-induced phonon generation for $\text{Pr}:\text{YAlO}_3$.

IV. ANALYSIS

We have tried to identify the origin of the magnetic field induced resonance in the dephasing time when the magnetic field is oriented along the c axis. To our knowledge only one case of a similar (but not identical) resonance in photon echo decay time as a function of magnetic field has been observed previously. This was in ruby ($\text{Cr}^{3+}:\text{Al}_2\text{O}_3$).²⁰ That resonance was much more strongly pronounced than the one observed in this paper, and was due to a magnetic-field induced crossing between hyperfine levels in the Cr^{3+} ion. As described below, a magnetic-field induced crossing between hyperfine levels does not appear to be the responsible mechanism for our case. Intensity drops of photon echo signals at magnetic-field-induced anti-crossings (avoided crossings) have been observed in the ${}^3H_4-{}^1D_2$ transition in Pr-doped YAlO_3 .²¹ However, at that time no effect on the photon echo decay rate at the avoided crossings could be observed. Our external magnet unfortunately is not strong enough for us to reach these anticrossings. It would otherwise be interesting to see if there would be a discernible effect on the dephasing time at sufficiently low excitation energy. To calculate the position of the energy levels and the expected level crossing points as a function of magnetic field, the Hamiltonian, H , in Eq. (3.8) in Ref. 21 was used.

$$H = B(\gamma_X \sin\theta \cos\phi + \gamma_Y \sin\theta \sin\phi + \gamma_Z \cos\theta) + D \left(I_Z^2 - \frac{I(I+1)}{3} \right) + E(I_X^2 - I_Y^2). \quad (2)$$

The first term is the nuclear Zeeman effect. γ_X , γ_Y , and γ_Z are the effective enhanced nuclear gyromagnetic ratios in Eq. (2.11) of Ref. 5, B is the magnetic field, θ is the angle between the magnetic field and the principal axis (Z axis) for the nuclear quadrupole tensor of the Pr ion and ϕ is the angle between the nuclear quadrupole tensor X axis and the projection of the magnetic field on the XY plane. The coupling constants D and E depend on the nuclear electric quadrupole interactions and the second order hyperfine and electronic Zeeman effects.⁵ I is the total nuclear spin ($\frac{5}{2}$ for Pr and Al) and I_X , I_Y , and I_Z are nuclear spin operators.²¹ The Pr: YAlO_3 data on page 111 in Ref. 5 for D , E , γ_X , γ_Y , and γ_Z was used to calculate the energy of the Pr hyperfine levels in the ground and excited states versus magnetic field. The principal axis (the Z axis) for the nuclear quadrupole tensor of the Pr ion lies in a plane perpendicular to the crystal c axis for the 3H_4 as well as for the 1D_2 state as can be found in Refs. 21–23. The X axis of the quadrupole tensor is assumed to be oriented along the crystal c axis. The Z axis of the two nonequivalent Pr sites are symmetrically oriented with respect to the crystal b axis. The angles between the crystal b axis and the quadrupole tensor z axes are 56.4° and 69.2° for the 3H_4 and 1D_2 states, respectively.²³ We have calculated the Pr Zeeman sublevels for the two non equivalent Pr sites under different magnetic field orientations corresponding to

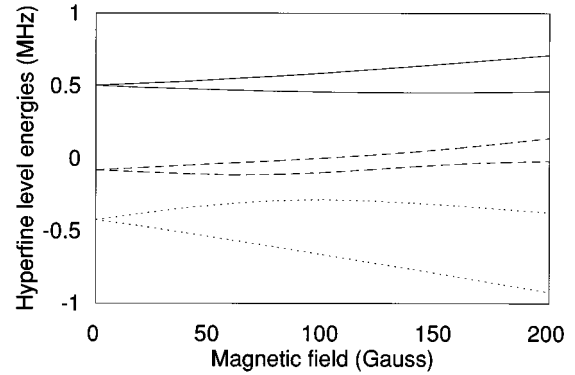


FIG. 6. Sample calculation of the Al hyperfine sublevel energies versus magnetic field. The magnetic field is oriented parallel to the c axis. $|m_l| = \frac{5}{2}$ (solid lines), $|m_l| = \frac{3}{2}$ (dashed lines), $|m_l| = \frac{1}{2}$ (dotted lines).

the conditions during our experiments. It turns out that for magnetic fields below 15 mT there are no crossings or anti-crossings in neither the 3H_4 nor the 1D_2 state. (The effective enhanced nuclear gyromagnetic ratio, Γ_x , for the 1D_2 state was in this calculation assumed to be equal to 14.8 MHz/T,⁵ but there are no reasonable values for Γ_x that give a crossing in the region that we have investigated experimentally.) A difference between the parallel and the perpendicular cases is that in the former case the $\frac{5}{2}$ Zeeman sublevels are almost degenerate for the 3H_4 state and the splitting is very small for the 1D_2 state while in the latter alternative all the Zeeman sublevels are separated.

Hyperfine crossings in Pr thus did not appear to be the reason for the resonance. An alternative possibility for the observed behavior could be magnetic-field-induced hyperfine crossings in the host lattice Al ions. We are not aware of any previous observations of such an effect in these kinds of system but it is certainly conceivable that the increased host ion nuclear spin-flip rate that could result from such a crossing might induce an increased dephasing also for a dopant ion. Again, as in the Pr case mentioned above, the energy levels can be calculated as a function of magnetic field from Eq. (2). Values for the nuclear quadrupole coupling parameter, the asymmetry, and gyromagnetic ratios were taken from Ref. 24 and adapted to Eq. (2) above.²⁵ The angles between the quadrupole tensor and the crystal axis were obtained from Ref. 26. There are four Al sites in the YAlO_3 crystal. Simulations for all four Al sites under the magnetic-field orientations mentioned above have been performed. Again no crossing exists for magnetic fields below 15 mT. An example of an Al hyperfine structure diagram is shown in Fig. 6.

Another possible cause of the increased dephasing that we have considered is energy transfer between the Pr atoms and the crystal host atoms due to an accidental coincidence of hyperfine level transition frequencies at the resonance field. This would then occur through mutual nuclear spin flips of host atoms and the Pr ions. The most likely host ion candidate for such a transfer again are the Al ions since the O atoms have zero nuclear moments and the nuclear moment of ytterbium is only about 5% of the aluminium nuclear moment. The authors have examined all combinations of the

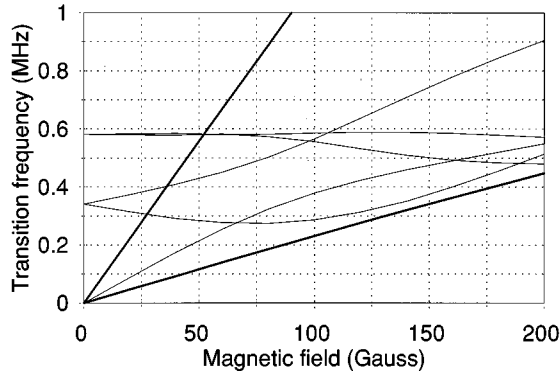


FIG. 7. Calculation of the frequencies for the nuclear spin $\Delta m_I = \pm 1$ hyperfine transitions for one of the Al ion sites are shown together with the frequencies of the hyperfine transitions between the Pr $m_I = +\frac{1}{2}$ and $m_I = -\frac{1}{2}$ levels in the upper as well as the lower electronic state (thick lines).

two Pr sites, the four Al sites for various magnetic field orientations. In Fig. 7, one example of such a calculation is given. The frequencies for the nuclear spin $\Delta m_I = \pm 1$ hyperfine transitions in the Al ions (thin lines) are shown together with the frequencies of the hyperfine transitions between the Pr $m_I = +\frac{1}{2}$ and $m_I = -\frac{1}{2}$ levels in the 3H_4 ground state as well as in the 1D_2 excited state (thick lines). Other hyperfine transitions in Pr occur at frequencies that are higher than the Al hyperfine transition frequencies. Clearly there are coincidences both between the Pr and Al hyperfine transition frequencies and between Al hyperfine frequencies themselves. However, if diagrams of the type shown in Fig. 7 are drawn for increasing angle between the magnetic field and the c axis, a transition from a sharp resonance as a function of magnetic field (Fig. 3) into a more shallow and less pronounced structure as the angle between the crystal c axis and the magnetic field increases, cannot be inferred from the calculations.

Thus in all we have no satisfactory explanation for the observed resonance at this time. We believe a good way for identifying the origin of the resonance would be to perform optically detected magnetic resonance experiments. To observe the hyperfine levels as a function of magnetic field

would require a tuneable radio frequency source. This equipment is unfortunately not available in our laboratory at this time so we are presently unable to perform such experiments. Still, since we are not aware of other observations of the type of resonance observed in this paper we report our results in their current form.

V. CONCLUSIONS

Two-pulse photon echo intensity versus pulse separation have been measured at liquid helium temperatures in the 3H_4 - 1D_2 transition of $\text{Pr}^{3+}:\text{YAIO}_3$ as a function of magnetic field for different excitation pulse energies. When the magnetic field was oriented along, or at a small angle to the crystal c axis, a resonance in the photon echo decay time as a function of magnetic field was observed at low excitation energies. At higher pulse energies, excitation energy-dependent dephasing masked the resonance. This demonstrates the importance of extrapolating dephasing measurements towards zero energy. Not only is this necessary in order to determine a true intrinsic homogeneous linewidth but also additional subtle interactions can be masked by excitation energy-dependent dephasing processes. We believe that the most likely cause of the resonance would be a Zeeman level crossing or a coincidence between transition frequencies between the hyperfine levels. Previous observations of such types of resonances have been scarce but we have knowledge of at least one partly similar case.²⁰ However, based on known data for the crystal, the cause of the resonance observed in this work could not be positively identified.

ACKNOWLEDGEMENTS

This work has been supported by the Swedish Natural Science Research Council and the Crafoord foundation. We would like to thank Professor M. Aldén for lending us the laser system. The general support of this project by Professor S. Svanberg is also gratefully acknowledged. The $\text{Pr}:\text{YAIO}_3$ crystal was borrowed from Dr. Ravinder Kachru at SRI International. S.K. also wishes to thank Dr Kachru for several helpful discussions and Professor V. Samartsev at Kazan Physio-Technical Institute, Russia, for verifying some of the calculations.

¹W. E. Moerner, *Persistent Spectral Hole-Burning: Science and Applications* (Springer, New York, 1988), Chap. 7, pp. 251–307.

²F. M. Schellenberg, W. Lenth, and G. C. Bjorklund, *Appl. Opt.* **25**, 3207 (1986).

³T. W. Mossberg, *Opt Lett.* **7**, 77 (1982).

⁴R. W. Equal, Y. Sun, R. L. Cone, and R. M. Macfarlane, *Phys. Rev. Lett.* **72**, 2179 (1994).

⁵R. M. Macfarlane and R. M. Shelby, in *Spectroscopy of Solids Containing Rare Earth Ions*, edited by A. A. Kaplyanskii and R. M. Macfarlane (Elsevier, New York, 1987).

⁶R. M. Macfarlane, R. M. Shelby, and R. L. Shoemaker, *Phys. Rev. Lett.* **43**, 1726 (1979).

⁷J. Huang, J. M. Zhang, A. Lezama, and T. W. Mossberg, *Phys. Rev. Lett.* **63**, 78 (1989).

⁸G. K. Liu and R. L. Cone, *Phys. Rev. B* **41**, 6193 (1990).

⁹S. Kröll, E. Y. Xu, and R. Kachru, *Phys. Rev. B* **44**, 30 (1991).

¹⁰Y. S. Bai and R. Kachru, *Phys. Rev. B* **46**, 13 735 (1992).

¹¹S. B. Altner, M. Mitsunaga, G. Zumofen, and U. P. Wild, *Phys. Rev. Lett.* **76**, 1747 (1996).

¹²R. W. Equall, R. L. Cone, and R. M. Macfarlane, *Phys. Rev. B* **52**, 3963 (1995).

¹³M. Mitsunaga, T. Takagahara, R. Yano, and N. Uesugi, *Phys. Rev. Lett.* **68**, 3216 (1992).

¹⁴S. Kröll, E. Y. Xu, M. K. Kim, R. Kachru, and M. Mitsunaga,

- Phys. Rev. B **41**, 11 568 (1990).
- ¹⁵M. Mitsunaga, R. Yano, and U. Uesugi, Phys. Rev. B **45**, 12 760 (1992).
- ¹⁶J. Huang, J. M. Zhang, and T. W. Mossberg, Opt. Commun. **75**, 29 (1990).
- ¹⁷R. M. Macfarlane and R. M. Shelby, Opt. Commun. **39**, 169 (1981).
- ¹⁸R. M. Shelby and R. M. Macfarlane, Phys. Rev. Lett. **45**, 1098 (1980).
- ¹⁹L. Root and J. L. Skinner, Phys. Rev. B **32**, 4111 (1985).
- ²⁰L. Q. Lambert, Phys. Rev. B **7**, 1834 (1973).
- ²¹A. Wokaun, S. C. Rand, R. G. DeVoe, and R. G. Brewer, Phys. Rev. B **23**, 5733 (1981).
- ²²L. E. Erickson, Phys. Rev. B **19**, 4412 (1979).
- ²³M. Mitsunaga, E. S. Kintzer, and R. G. Brewer, Phys. Rev. B **31**, 6947 (1985).
- ²⁴D. P. Burum, R. M. Macfarlane, and R. M. Shelby, Phys. Lett. A **90**, 483 (1982).
- ²⁵A. Abragam, *The Principles of Nuclear Magnetism* (Clarendon Oxford, 1961), Chap. VII, Eq. (22).
- ²⁶D. P. Burum, R. M. Macfarlane, R. M. Shelby, and L. Mueller, Phys. Lett. A **91**, 465 (1982).